

Published in final edited form as:

*Atherosclerosis*. 2012 May ; 222(1): 129–134. doi:10.1016/j.atherosclerosis.2012.02.029.

## Association of pericardial fat and coronary high-risk lesions as determined by cardiac CT

Christopher L. Schlett<sup>a,b</sup>, Maros Ferencik<sup>a,c</sup>, Matthias F. Krieger<sup>a</sup>, Fabian Bamberg<sup>e</sup>, Brian B. Ghoshhajra<sup>a,b</sup>, Subodh B. Joshi<sup>a</sup>, John T. Nagurney<sup>d</sup>, Caroline S. Fox<sup>f,g</sup>, Quynh A. Truong<sup>a,c</sup>, and Udo Hoffmann<sup>a,b,\*</sup>

<sup>a</sup>Cardiac MR, PET, CT Program, Massachusetts General Hospital and Harvard Medical School, Boston, MA, USA

<sup>b</sup>Department of Radiology, Massachusetts General Hospital and Harvard Medical School, Boston, MA, USA

<sup>c</sup>Cardiology Division, Massachusetts General Hospital and Harvard Medical School, Boston, MA, USA

<sup>d</sup>Department of Emergency Medicine, Massachusetts General Hospital and Harvard Medical School, Boston, MA, USA

<sup>e</sup>Department of Clinical Radiology, Ludwig-Maximilians University, Klinikum Grosshadern, Marchioninistrasse 15, 81377 Munich, Germany

<sup>f</sup>National Heart, Lung and Blood Institute's Framingham Heart Study, Framingham, MA, USA

<sup>g</sup>Division of Endocrinology, Metabolism, and Diabetes, Department of Medicine, Brigham and Women's Hospital and Harvard Medical School, Boston, MA, USA

### Abstract

**Objective**—Pericardial adipose tissue (PAT) is a pathogenic fat depot associated with coronary atherosclerosis and cardiovascular events. We hypothesized that higher PAT is associated with coronary high-risk lesions as determined by cardiac CT.

**Methods**—We included 358 patients (38% female; median age 51 years) who were admitted to the ED with acute chest pain and underwent 64-slice CT angiography. The cardiac CT data sets were assessed for presence and morphology of CAD and PAT. Coronary high-risk lesions were defined as >50% luminal narrowing and at least two of the following characteristics: positive remodeling, low-density plaque, and spotty calcification. PAT was defined as any pixel with CT attenuation of –190 to –30 HU within the pericardial sac.

**Results**—Based on cardiac CT, 50% of the patients ( $n = 180$ ) had no CAD, 46% ( $n = 165$ ) had CAD without high-risk lesions, and 13 patients had CAD with high-risk lesions. The median PAT in patients with high-risk lesions was significantly higher compared to patients without high-risk lesions and without any CAD (151.9 [109.0–179.4] cm<sup>3</sup> vs. 110.0 [81.5–137.4] cm<sup>3</sup>, vs. 74.8 [58.2–111.7] cm<sup>3</sup>, respectively  $p = 0.04$  and  $p < 0.0001$ ). These differences remained significant after adjusting for traditional risk factors including BMI (all  $p < 0.05$ ). The area under the ROC

© 2012 Elsevier Ireland Ltd. All rights reserved.

\*Corresponding author at: Cardiac MR, PET, CT Program, Department of Radiology Massachusetts General Hospital and Harvard Medical School, Boston, MA 02114, USA. Tel.: +1 617 726 1255; fax: +1 617 724 4152. uhoffmann@partners.org (U. Hoffmann).

#### Conflict of interest

None of the authors have any competing financial interests in relation to the work described.

curve for the identification of high-risk lesions was 0.756 in a logistic regression model with PAT as a continuous predictor.

**Conclusion**—PAT volume is nearly twice as high in patients with high-risk coronary lesions as compared to those without CAD. PAT volume is significantly associated with high risk coronary lesion morphology independent of clinical characteristics and general obesity.

### Keywords

Coronary artery disease; Cardiac CT angiography; Pericardial fat; Adipose tissue; Vulnerable plaque; High-risk lesions

## 1. Introduction

Pericardial adipose tissue (PAT) is accurately and reproducibly quantified by cardiac computed tomography (CT) [1]. PAT volume is associated with cardiovascular risk factors, including blood glucose level, systolic blood pressure, and hypercholesterolemia [2,3]. In addition to storing lipids, PAT also secretes adipokines and proinflammatory cytokines such as tumor necrosis factor-alpha and interleukin-6 [4–8]. Because PAT directly surrounds the coronary arteries and shares the blood supply with the coronary artery wall, it is hypothesized that the secretion of cytokines may lead to an acceleration of atherosclerosis [9,10].

Cardiac CT can visualize coronary artery disease including lesion severity and plaque morphology by using contrast-enhanced scans [11,12]. This is particularly important as non-calcified and partially calcified plaques (mixed plaque) are associated with higher cardiovascular event rates than purely calcified lesions [13]. Additionally, the risk of acute coronary syndrome is increased if positive remodeling, low-attenuation plaque and/or spotty calcification are present [14–17]. The presence of two features (positive remodeling and low-attenuation plaque) has a high specificity (97%) for acute coronary syndrome (ACS) [15], which is validated in a prospective study [16]. Further, there is strong evidence that presence and extent of coronary atherosclerosis are associated with the amount of PAT [2,18,19]. More recently researchers have tried to demonstrate the association of PAT with plaque composition. The data indicates that higher PAT volumes are observed in patients with predominantly non-calcified plaque as compared to those with predominantly calcified plaques [20–22]. From this data [20,23,24], we hypothesized that increased PAT volume is associated with the presence of coronary high-risk lesions.

## 2. Methods

### 2.1. Study cohort

This is a sub-analysis of the “Rule Out Myocardial Infarction by Computed Tomography” (ROMICAT) trial, a cross-sectional, observational study. Briefly, 368 consecutive adult patients were enrolled, who were admitted presented to the ED with acute chest pain. These patients were hemodynamically stable, had normal or non-diagnostic electrocardiogram (ECG), and negative initial cardiac biomarkers. All patients underwent a cardiac multi-detector CT exam. A major exclusion criterion was previously known CAD (prior stent placement, or bypass grafting). More details were provided elsewhere [25]. Furthermore, patients were excluded from this sub-analysis ( $N=10$ ), if image quality was low and did not allow quantitative fat or plaque assessment or if major co-variables were missing. All participants provided written informed consent and the Institutional Review Board of the Massachusetts General Hospital approved the study.

## 2.2. CT scan protocol

The used CT scan protocol was described in detail elsewhere [25]. Briefly, all CT imaging was performed with a 64-slice multi-detector CT scanner (Sensation 64, Siemens Medical Solutions, Forchheim, Germany). Imaging parameters included slice collimation: 64 mm × 0.6 mm, gantry rotation time: 330 ms, tube voltage: 120 kV, effective tube current: 850–950 mA s depending on patient body size. Contrast injection (Nycomed Amersham GE-Healthcare Vispaque 300 mg/mL) was administered at an injection rate of 5 mL per second with a delay calculated during the timing bolus scan. Overlapping transaxial images were reconstructed using a medium sharp convolution kernel (B25f) with an image matrix of 512 × 512 pixels, slice thickness and increment of 0.75/0.4 mm using an electrocardiogram gated half-scan algorithm. Image reconstruction was retrospectively gated to the electrocardiogram.

## 2.3. Peri-cardial fat measurements

Reconstructed CT data sets of all patients were transferred to an offline workstation (Leonardo, Siemens Medical Solutions). The volume of Pericardial Adipose Tissue (PAT) was measured using a threshold based method. An attenuation of –190 to –30 HU was corresponding to adipose tissue in contrast enhanced cardiac CT scans [1]. PAT was defined as any pixel within these attenuation thresholds inside the pericardial sac. A region of interest was manually drawn following the pericardial sac, starting at the mid-level of the right pulmonary artery. The contour was drawn every one centimeter and interpolated in between with a dedicated software program (Volume Viewer, Siemens Medical Solutions, Forchheim, Germany). If necessary the interpolated contours were manually adjusted. PAT was measured in cubic centimeters (cm<sup>3</sup>). This approach has been described and validated previously to have an excellent inter- and intra-observer reproducibility (intraclass correlation coefficient of 0.98 and 0.99, respectively) [1].

## 2.4. Assessment of coronary artery disease

Reconstructed CT image sets of all patients were transferred to an offline workstation (Leonardo; Siemens Medical Solutions, Forchheim, Germany), and evaluated for the presence of coronary plaque as well the presence of obstructive disease (luminal narrowing of >50%) for each segment of the coronary artery tree, using a 17-segment model. Excellent inter-reader reliability was previously reported for this assessment [26]. CAD and PAT were assessed done independently and readers were blinded to the clinical variables and other CT results.

Patients with obstructive disease (>50% luminal narrowing) were further evaluated regarding their severity and morphology of the stenosis. If more than one stenosis was present in a patient, the most severe lesion was analyzed. Each lesion was analyzed in curved multiplanar reformatted images in long axis and cross-sectional views using a dedicated workstation (Vitrea, Vital Images, Minnetonka, MN). With a semi-automated software (Vessel Probe, Vitrea, Vital Images, Minnetonka, MN) lumen and outer vessel boundaries were segmented and manually adjusted if necessary.

The diameters at the site of the maximum stenosis and at the proximal and distal references were measured. The remodeling index was calculated as the outer vessel diameter at the site of the maximum stenosis divided by the mean of the outer vessel diameters at the proximal and distal references. Positive remodeling was defined as a remodeling index of >1.05 [27]. The plaque volume was automatically calculated as the volume of all segmented voxels between the luminal and outer vessel boundaries in curved multiplanar reformatted images. At the site of the lesion, we reported the total plaque volume and plaque volume with CT attenuation <30 HU, so-called low-attenuation plaque. If more than 10% of the entire lesion

consistent of plaque <30 HU, the lesion was considered as positive for low-attenuation, similar to the approach proposed by Marwan et al. [28]. The composition of the plaque was assessed visually and categorized as calcified and non-calcified plaques as described previously [11]. In the presence of coronary calcification, calcified plaques were further characterized as spotty calcifications if discrete calcified nodules were present (less than 3 mm in diameter), which were clearly surrounded by non-calcified plaque [15].

A lesion was defined as high-risk if at least two of the following lesion characteristics were present: spotty calcification, positive remodeling, and low-attenuation plaque.

## 2.5. Clinical covariates

Hypertension was defined as systolic blood pressure  $\geq 140$  mmHg, diastolic blood pressure  $\geq 90$  mmHg, or the use of antihypertensive medication. Hypercholesterolemia was defined as total cholesterol  $> 200$  mg/dL or the use of a cholesterol-lowering agent. Patients were classified as smoking if they had smoked at least one cigarette per day in the year before the study. Family history of CAD was defined as having a first degree female ( $< 65$  years) or male ( $< 55$  years) relative with a documented history of myocardial infarction or sudden death. Obesity was defined as a BMI  $\geq 30$  kg/m<sup>2</sup>. Patients were classified as high-risk ( $> 20\%$ ), intermediate (10–20%), or low-risk ( $< 10\%$ ) according to their Framingham risk score [29].

## 2.6. Statistical analysis

Continuous measures were summarized by median [interquartile range] and categorical by percentage (counts) unless otherwise specified. To assess whether PAT volume was significantly different between categories of CAD and categories of the included covariates, Wilcoxon signed-rank test was applied for binary variables, and Kruskal–Wallis test for variables with more than two categories. Since age was not linearly correlated to PAT (age [3]:  $p = 0.03$ ), age was categorized into groups with similar intervals of PAT between the age-groups in univariate analysis to use it as an ordinal variable in all further analysis.

For multivariate analysis, Quantile regression was used to calculate adjusted differences in median levels and a Markov chain marginal bootstrap algorithm to determine 95% confidence intervals (95%CI) and  $p$ -values [30]. Co-variables were included into the model if they demonstrated a significance level  $p < 0.10$  in univariate analysis. As a sub-analysis, we adjusted the association of PAT and high-risk lesions in addition for the overall plaque burden, which was measured as the number of coronary segments containing any atherosclerotic plaque.

The diagnostic utility of PAT for the detection of patients with coronary high-risk lesions was assessed using  $c$ -statistics, which is equivalent to the area under the receiver-operating characteristics (ROC) curve (AUC). The asymptotic 95%CI for the AUCs were estimated using a nonparametric approach which is closely related to the jackknife technique. Logistic regression analysis was performed to calculate odds ratios with 95%CI for the prediction of high-risk lesions by each standard deviation of PAT. Based on the ROC two PAT cut-points were derived, one optimizing the AUC and one with 100% sensitivity for a coronary high-risk lesion. Finally, diagnostic accuracy of PAT cut-points (sensitivity, specificity, negative predictive value [NPV], positive predictive value [PPV]; plus binomial 95%CI) was calculated for the presence high-risk lesions.

All performed tests were two-sided and a  $p$ -value  $< 0.05$  was considered as statistically significant. All analyses were performed with SAS (version 9.2, SAS Institute Inc., Cary, NC USA).

### 3. Results

Within the study cohort ( $n = 358$ , 38% female, median age 51 [IQR 45–59] years), the median amount of PAT was 95.2 [IQR 66.0–130.1]  $\text{cm}^3$ . Most of the patients were at low to intermediate cardiovascular risk according to the Framingham Risk Score (Table 1). PAT volume was higher in patients, who were male ( $p = 0.001$ ), older ( $p < 0.0001$ ), obese ( $p < 0.0001$ ), and in patients with hypertension ( $p < 0.0001$ ), hypercholesterolemia ( $p < 0.0001$ ), or diabetes ( $p = 0.006$ ). Smoking was not associated with PAT ( $p = 0.11$ ).

Based on cardiac CT, 180 patients (50%) had no CAD. Of the remaining 178 patients, 93% ( $n = 165$ ) had CAD without high-risk lesions, and 7% ( $n = 13$ ) had a high risk-lesion (Table 1). Of these 13 patients, all had significant stenosis and five had all three features of high-risk plaque (positive remodeling, spotty calcification and low-attenuation plaque; as shown in Fig. 1) while eight patients had only two of the three features (3 $\times$  positive remodeling/spotty calcification; 3 $\times$  positive remodeling/low-attenuation plaque; 2 $\times$  low-attenuation plaque/spotty calcification).

#### 3.1. Pericardial fat and CAD

The median PAT volume was nearly 50% higher in patients with CAD as compared to patients without CAD (111.7 [IQR 84.5–145.23]  $\text{cm}^3$  vs. 74.8 [IQR 58.2–111.7]  $\text{cm}^3$ ,  $p < 0.0001$ ), Fig. 2. This difference remained statistically significant after multivariate adjustment for gender, age, hypertension, hyperlipidemia, diabetes and BMI ( $p = 0.002$ ). After multivariate adjustment, the estimated difference in median PAT volumes was 19.7 [95% CI 7.4–31.9]  $\text{cm}^3$  between patients with and without CAD, Table 2. This difference in PAT between these subgroups remained similar if patients with high-risk lesions were excluded from the analysis (18.8 [95% CI 3.9–33.6]  $\text{cm}^3$ ).

#### 3.2. Pericardial fat and coronary high-risk lesion morphology

In patients with high-risk lesions, the median level of PAT was 151.9 [IQR 109.0–179.4]  $\text{cm}^3$ . This was significantly higher as compared to patients with CAD but without high-risk lesions (110.0 [IQR 81.5–137.4]  $\text{cm}^3$ ,  $p = 0.04$ ) and more than twice as high as compared to patients without CAD ( $p < 0.0001$ ), Fig. 3. These differences remained statistically significant after multivariate adjustment for cardiovascular risk factors (all  $p < 0.05$ ), Table 2. Importantly, the difference in PAT volume between patients with CAD but without high-risk lesions and those with high-risk lesions was statistically independent of plaque burden ( $p = 0.02$ ).

#### 3.3. Discriminatory value of pericardial fat for coronary high-risk lesion morphology

For each standard deviation of PAT volume (49.8  $\text{cm}^3$ ), the odds for the presence of high-risk lesion increased nearly two-fold (OR 1.79 [95% CI: 1.16–2.76],  $p = 0.008$ ). PAT volume was well discriminative for high-risk lesions (AUC 0.756 [95% CI: 0.644–0.867]), Fig. 4. At a cut-point optimized for maximal AUC (PAT volume: 144.88  $\text{cm}^3$ ), the sensitivity for high-risk lesions was 62% [95% CI: 32–86%] and the specificity was 84% [95% CI: 79–87%]. Among patients with CAD, the sensitivity was similar at 62% [95% CI: 32–86%] while the specificity was slightly lower at 77% [95% CI: 70–83%], Table 3. A PAT volume below 74.07  $\text{cm}^3$  excluded the presence of coronary high-risk lesions, Table 3.

### 4. Discussion

PAT volume is nearly twice as high in patients with coronary high-risk lesions as compared to those without CAD. PAT volume is significantly associated with high risk coronary lesion morphology. These associations were statistically independent of clinical

characteristics, including measures of obesity and cardiovascular risk factors as well as the extent of CAD. Low PAT volumes excluded the presence of high risk coronary lesion morphology.

#### 4.1. Association of pericardial fat to coronary artery disease

We detected sizable differences not only between the patients with high-risk lesions and those without any CAD (more than twice the volume of PAT), but also between patients with high-risk lesions and patients with CAD but without high-risk lesions. Remarkably, these findings were statistically independent of traditional measures of obesity and cardio-metabolic risk profile. Furthermore, we also showed that this association was not predominantly driven by patients with high-risk lesions, since the estimated difference remained similar after excluding those patients. These findings complement prior studies demonstrating that higher PAT volume is related to reduced coronary blood flow [31], myocardial ischemia, and cardiovascular events [32–34]. More important, our results extended these findings regarding vulnerability of coronary plaque, as detailed below. The results also strongly suggest a local proatherogenic effect of PAT [4], although our study design did not allow assessing the associations of visceral abdominal fat (VAT) measured by CT or waist circumference, which is a clinical measure of abdominal obesity with PAT. However, previous studies showed that the association of PAT with CAD was independent of VAT [32,35]. Our data supports the consideration of PAT as a new imaging based risk factor for CAD incremental to traditional cardio-metabolic or obesity measures [36].

#### 4.2. Association of pericardial fat to plaque vulnerability

Our results extend previous observations that PAT is associated with the presence [2,18,19,37–39] and composition [20,22] of coronary atherosclerosis as we demonstrate the association of PAT with a specific coronary high-risk lesion morphology. The median PAT volume difference was statistically independent of traditional cardiovascular risk factors (including BMI), but also statistically independent of the extent of plaque burden. This is important because it eliminates plaque burden as a confounding factor and generates and supports the hypothesis of a local effect of PAT on coronary atherosclerosis. It is important to note for potential clinical implications that that low PAT volumes ( $<74.08 \text{ cm}^3$ ) completely excluded the presence of coronary high-risk lesion morphology (NPV: 100%; 95% CI: 97–100%). If validated in large outcome studies and easily available in the future PAT may be used as additional information for risk stratification. Our results are supported by the previous observations that found an independent association of PAT volume to low-density plaque as well positive remodeling [24]. In their study, they used a cut-point of  $100 \text{ cm}^3$  PAT volume, which led to a sensitivity and specificity of 80% and 41% for the prediction of high-risk plaque, respectively. While we derived a higher cut-point ( $144.88 \text{ cm}^3$ ), the diagnostic accuracy for high risk lesions was comparable to the study of Oka et al. [24]. Further support for our hypothesis stems from an IVUS study in 108 patients which demonstrated that thickness of pericardial fat, as measured by transthoracic echocardiography, was independently associated to positive remodeling, as defined by IVUS [40]. Those observed associations between PAT and coronary plaque vulnerability may be explained by the inflammatory capacity of PAT, which secretes several pro-inflammatory cytokines [4]. Further, higher inflammation, as measured by positron emission tomography, was observed not only in culprit carotid plaque, but also in coronary plaque and predicted future events [41,42]. The pro-inflammatory role of PAT provides the most convincing pathophysiological explanation for our observed association to plaque vulnerability.

#### 4.3. Limitations

This is a cross sectional study and only associations but no causality can be derived from the results. Our cohort was recruited from an acute chest pain population presenting to the

emergency department and the results may not be fully generalizable to an asymptomatic population. Furthermore, our subgroup of patients with high-risk lesions is limited in sample size and validation of the derived cut-off values in a larger cohort is advisable. Detailed plaque morphology assessment was only performed in patients with a stenotic lesion, although events can also occur in non-stenotic lesions. While our definition for high-risk lesions was based on the findings of Motoyama et al. [15], there is no universal consensus on a CT based definition of vulnerable or high risk plaque and further studies are needed to define the association of these findings and subsequent cardiac events. Given the growing body of evidence suggesting that PAT may be an important measurement, it appears that standardization of PAT measurements is warranted, which includes exact definition of anatomic landmarks and HU range. Such standardization is currently missing and may explain some differences between published reports.

## 5. Conclusion

In patients with high-risk lesions, PAT volume is higher as compared to patients with CAD but no high-risk lesions and as compared to patients with no CAD. All associations were independent of clinical characteristics and BMI. PAT volume has further a strong discriminative power for, while PAT volume below 74 cm<sup>3</sup> made high-risk lesions unlikely.

## References

1. Nichols JH, Samy B, Nasir K, et al. Volumetric measurement of pericardial adipose tissue from contrast-enhanced coronary computed tomography angiography: a reproducibility study. *Journal of Cardiovascular Computed Tomography*. 2008; 2:288–95. [PubMed: 19083964]
2. Rosito GA, Massaro JM, Hoffmann U, et al. Pericardial fat, visceral abdominal fat, cardiovascular disease risk factors, and vascular calcification in a community-based sample: the Framingham Heart Study. *Circulation*. 2008; 117:605–13. [PubMed: 18212276]
3. Wang CP, Hsu HL, Hung WC, et al. Increased epicardial adipose tissue volume in type 2 diabetes mellitus and association with metabolic syndrome and severity of coronary atherosclerosis. *Clinical Endocrinology*. 2008
4. Iacobellis G, Barbaro G. The double role of epicardial adipose tissue as pro-and anti-inflammatory organ, Hormone and metabolic research = Hormon- und Stoffwechselforschung = Hormones et métabolisme. 2008; 40:442–5. [PubMed: 18401833]
5. Mazurek T, Zhang L, Zalewski A, et al. Human epicardial adipose tissue is a source of inflammatory mediators. *Circulation*. 2003; 108:2460–6. [PubMed: 14581396]
6. Baker AR, Silva NF, Quinn DW, et al. Human epicardial adipose tissue expresses a pathogenic profile of adipocytokines in patients with cardiovascular disease. *Cardiovascular Diabetology*. 2006; 5:1. [PubMed: 16412224]
7. Cheng KH, Chu CS, Lee KT, et al. Adipocytokines and proinflammatory mediators from abdominal and epicardial adipose tissue in patients with coronary artery disease. *International Journal of Obesity* 2008. 2005; 32:268–74.
8. Pou KM, Massaro JM, Hoffmann U, et al. Visceral and subcutaneous adipose tissue volumes are cross-sectionally related to markers of inflammation and oxidative stress: the Framingham Heart Study. *Circulation*. 2007; 116:1234–41. [PubMed: 17709633]
9. Fantuzzi G, Mazzone T. Adipose tissue and atherosclerosis: exploring the connection. *Arteriosclerosis, Thrombosis, and Vascular Biology*. 2007; 27:996–1003.
10. Yudkin JS, Eringa E, Stehouwer CD. Vasocrine” signalling from perivascular fat: a mechanism linking insulin resistance to vascular disease. *The Lancet*. 2005; 365:1817–20.
11. Achenbach S, Moselewski F, Ropers D, et al. Detection of calcified and non-calcified coronary atherosclerotic plaque by contrast-enhanced, submillimeter multidetector spiral computed tomography: a segment-based comparison with intravascular ultrasound. *Circulation*. 2004; 109:14–7. [PubMed: 14691045]

12. Achenbach S, Raggi P. Imaging of coronary atherosclerosis by computed tomography. *European Heart Journal*. 2010; 31:1442–8. [PubMed: 20484566]
13. Blankstein R, Ferencik M. The vulnerable plaque: can it be detected with Cardiac CT? *Atherosclerosis*. 2010; 211:386–9. [PubMed: 20619414]
14. Pundziute G, Schuijff JD, Jukema JW, et al. Evaluation of plaque characteristics in acute coronary syndromes: non-invasive assessment with multi-slice computed tomography and invasive evaluation with intravascular ultrasound radiofrequency data analysis. *European Heart Journal*. 2008; 29:2373–81. [PubMed: 18682447]
15. Motoyama S, Kondo T, Sarai M, et al. Multislice computed tomographic characteristics of coronary lesions in acute coronary syndromes. *Journal of the American College of Cardiology*. 2007; 50:319–26. [PubMed: 17659199]
16. Motoyama S, Sarai M, Harigaya H, et al. Computed tomographic angiography characteristics of atherosclerotic plaques subsequently resulting in acute coronary syndrome. *Journal of the American College of Cardiology*. 2009; 54:49–57. [PubMed: 19555840]
17. Kitagawa T, Yamamoto H, Horiguchi J, et al. Characterization of noncalcified coronary plaques and identification of culprit lesions in patients with acute coronary syndrome by 64-slice computed tomography. *JACC Cardiovascular Imaging*. 2009; 2:153–60. [PubMed: 19356549]
18. Ahn SG, Lim HS, Joe DY, et al. Relationship of epicardial adipose tissue by echocardiography to coronary artery disease. *Heart (British Cardiac Society)*. 2008; 94:e7. [PubMed: 17923467]
19. Gorter PM, de Vos AM, van der Graaf Y, et al. Relation of epicardial and pericoronary fat to coronary atherosclerosis and coronary artery calcium in patients undergoing coronary angiography. *The American Journal of Cardiology*. 2008; 102:380–5. [PubMed: 18678291]
20. Alexopoulos N, McLean DS, Janik M, Arepalli CD, Stillman AE, Raggi P. Epicardial adipose tissue and coronary artery plaque characteristics. *Atherosclerosis*. 2010; 210:150–4. [PubMed: 20031133]
21. Konishi M, Sugiyama S, Sugamura K, et al. Association of pericardial fat accumulation rather than abdominal obesity with coronary atherosclerotic plaque formation in patients with suspected coronary artery disease. *Atherosclerosis*. 2010; 209:573–8. [PubMed: 19892354]
22. Greif M, Becker A, von Ziegler F, et al. Pericardial adipose tissue determined by dual source CT is a risk factor for coronary atherosclerosis. *Arteriosclerosis, Thrombosis, and Vascular Biology*. 2009; 29:781–6.
23. Ueno K, Anzai T, Jinzaki M, et al. Increased epicardial fat volume quantified by 64-multidetector computed tomography is associated with coronary atherosclerosis and totally occlusive lesions. *Circulation Journal*. 2009; 73:1927–33. [PubMed: 19690390]
24. Oka T, Yamamoto H, Ohashi N, et al. Association between epicardial adipose tissue volume and characteristics of non-calcified plaques assessed by coronary computed tomographic angiography. *International Journal of Cardiology*. 2011
25. Hoffmann U, Bamberg F, Chae CU, et al. Coronary computed tomography angiography for early triage of patients with acute chest pain: the ROMICAT (Rule Out Myocardial Infarction using Computer Assisted Tomography) trial. *Journal of the American College of Cardiology*. 2009; 53:1642–50. [PubMed: 19406338]
26. Hoffmann U, Nagurney JT, Moselewski F, et al. Coronary multidetector computed tomography in the assessment of patients with acute chest pain. *Circulation*. 2006; 114:2251–60. [PubMed: 17075011]
27. Hoffmann U, Moselewski F, Nieman K, et al. Noninvasive assessment of plaque morphology and composition in culprit and stable lesions in acute coronary syndrome and stable lesions in stable angina by multidetector computed tomography. *Journal of the American College of Cardiology*. 2006; 47:1655–62. [PubMed: 16631006]
28. Marwan M, Taher MA, El Meniawy K, et al. In vivo CT detection of lipid-rich coronary artery atherosclerotic plaques using quantitative histogram analysis: a head to head comparison with IVUS. *Atherosclerosis*. 2011; 215:110–5. [PubMed: 21227419]
29. D'Agostino RB Sr, Vasan RS, Pencina MJ, et al. General cardiovascular risk profile for use in primary care: the Framingham Heart Study. *Circulation*. 2008; 117:743–53. [PubMed: 18212285]



30. He X, Hu F. Markov Chain Marginal Bootstrap. *Journal of the American Statistical Association*. 2002; 97:783–95.
31. Sade LE, Eroglu S, Bozbas H, et al. Relation between epicardial fat thickness and coronary flow reserve in women with chest pain and angiographically normal coronary arteries. *Atherosclerosis*. 2009; 204:580–5. [PubMed: 19019370]
32. Mahabadi AA, Massaro JM, Rosito GA, et al. Association of pericardial fat, intrathoracic fat, and visceral abdominal fat with cardiovascular disease burden: the Framingham Heart Study. *European Heart Journal*. 2009; 30:850–6. [PubMed: 19136488]
33. Janik M, Hartlage G, Alexopoulos N, et al. Epicardial adipose tissue volume and coronary artery calcium to predict myocardial ischemia on positron emission tomography-computed tomography studies. *Journal of Nuclear Cardiology*. 2010
34. Shmilovich H, Dey D, Cheng VY, et al. Threshold for the upper normal limit of indexed epicardial fat volume: derivation in a healthy population and validation in an outcome-based study. *The American Journal of Cardiology*. 2011
35. Bettencourt N, Toschke A, Leite D, et al. Epicardial adipose tissue is an independent predictor of coronary atherosclerotic burden. *International Journal of Cardiology*. 2011
36. Yerramasu A, Dey D, Venuraju S, et al. Increased volume of epicardial fat is an independent risk factor for accelerated progression of sub-clinical coronary atherosclerosis. *Atherosclerosis*. 2012; 220:223–30. [PubMed: 22015177]
37. Ding J, Kritchevsky SB, Hsu FC, et al. Association between non-subcutaneous adiposity and calcified coronary plaque: a substudy of the Multi-Ethnic Study of Atherosclerosis. *The American Journal of Clinical Nutrition*. 2008; 88:645–50. [PubMed: 18779279]
38. Jeong JW, Jeong MH, Yun KH, et al. Echocardiographic epicardial fat thickness and coronary artery disease. *Circulation Journal*. 2007; 71:536–9. [PubMed: 17384455]
39. de Vos AM, Prokop M, Roos CJ, et al. Peri-coronary epicardial adipose tissue is related to cardiovascular risk factors and coronary artery calcification in post-menopausal women. *European Heart Journal*. 2008; 29:777–83. [PubMed: 18156138]
40. Ogura R, Miyazaki S, Takahashi T, et al. Relationship between epicardial adipose tissue and coronary arterial remodeling as assessed by intravascular ultrasound in patients with coronary artery disease. *European Heart Journal*. 2011; S32:31–2.
41. Stolzmann P, Subramanian S, Abdelbaky A, et al. Complementary value of cardiac FDG PET and CT for the characterization of atherosclerotic disease. *Radiographics*. 2011; 31:1255–69. [PubMed: 21918043]
42. Menezes LJ, Kayani I, Ben-Haim S, Hutton B, Ell PJ, Groves AM. What is the natural history of 18F-FDG uptake in arterial atheroma on PET/CT? Implications for imaging the vulnerable plaque. *Atherosclerosis*. 2010; 211:136–40.

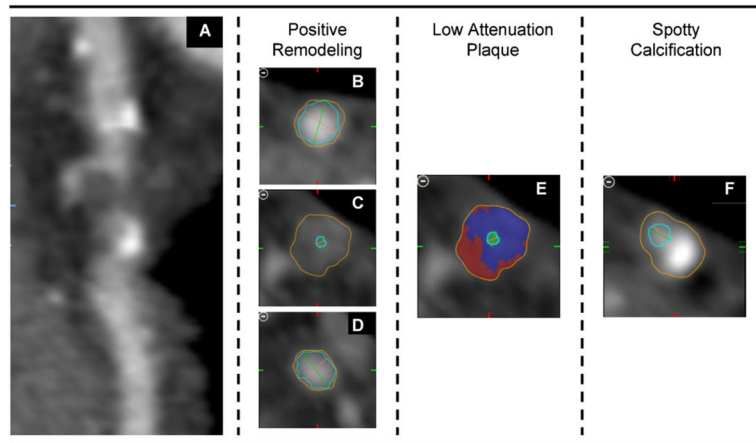


**Fig. 1.**

Coronary CT images of one patient with a high-risk Lesion. Curved Multi-planar Reconstructed images (A) demonstrated a coronary lesion with >50% luminal narrowing and all three high-risk features. Quantitative analysis assessing outer wall dimensions (orange line in: B, proximal reference; C, at the lesion; D, distal reference) yield a positive remodeling index of greater than 1.05. Volumetric measurements of the entire lesion demonstrated 28.5% low attenuation plaque (attenuation <30 HU, red super imposed in a representative, cross-sectional image [E]). Further, a spotty calcification (<3 mm) was adjunct to the lesion (F). If at least two of the three plaque features were present at the site of a coronary lesion, it was considered as high-risk lesion. (For interpretation of the references to color in this figure legend, the reader is referred to the web version of the article.)

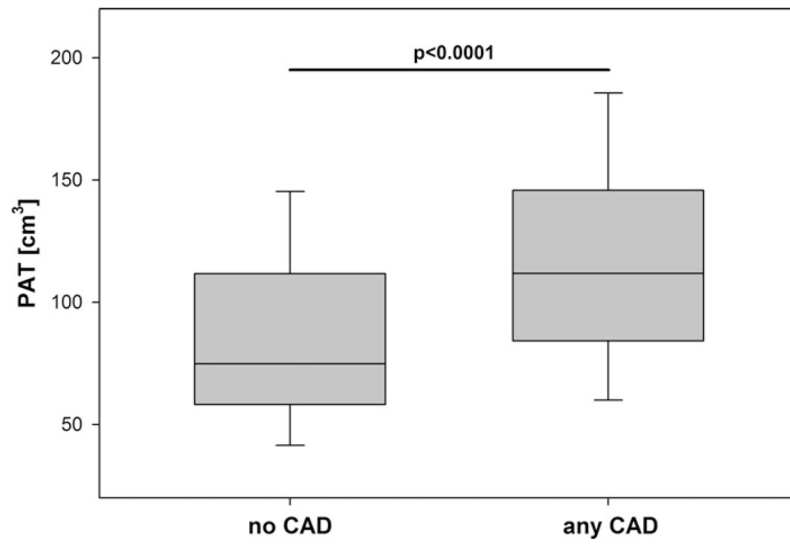


**Fig. 2.** Median levels of pericardial adipose tissue (PAT) between patients with and without any CAD.

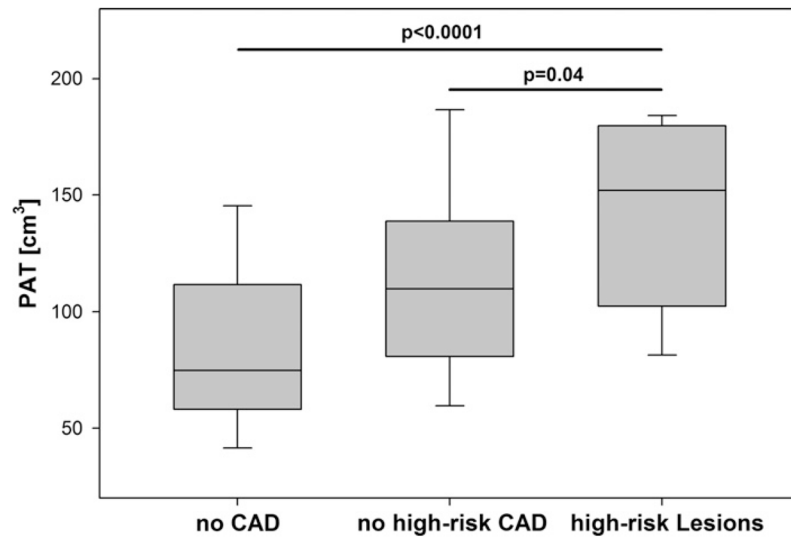


**Fig. 3.** Median levels of pericardial adipose tissue (PAT) between patients with no CAD, with no high-risk CAD and with high-risk lesions.

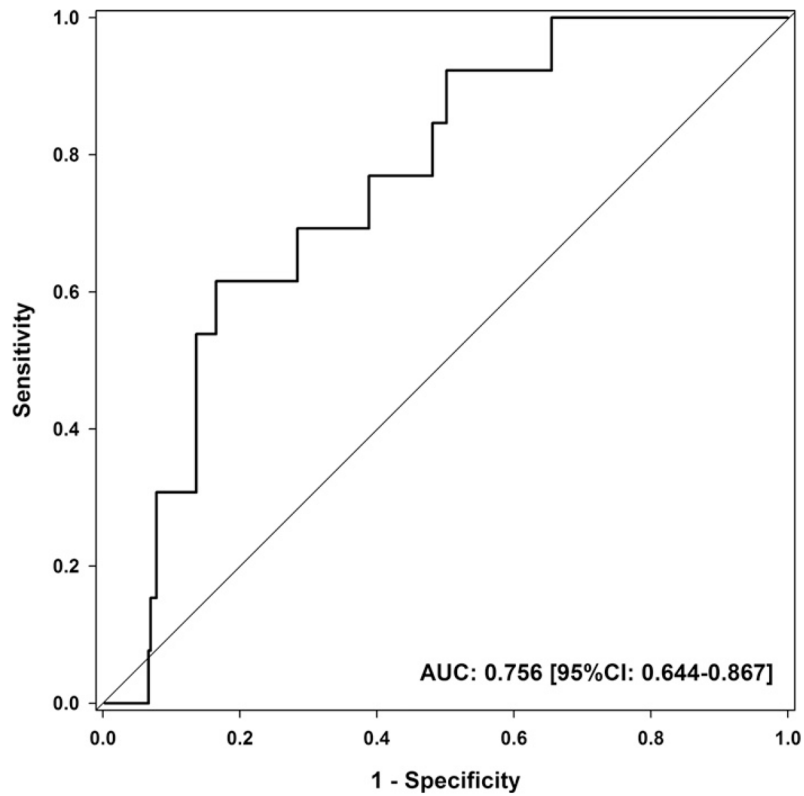


**Fig. 4.** ROC curve of pericardial adipose tissue (PAT) to predict high-risk lesions as defined by coronary CT angiography. In total, 13 patients were identified with a stenotic lesion which had at least two of the following high-risk features: spotty calcification, positive remodeling, low-attenuation plaque.

**Table 1**

Patients demographics. Framingham risk score [FRS] was missing for 4 patients. IQR: interquartile range; CAD: coronary artery disease; BMI: body-mass-index.

Variables	Median [IQR] or % [N]
CAD burden	
No CAD	50% [180]
No high-risk CAD	46% [165]
High-risk lesions	4% [13]
Age (years)	51 [45–59]
Gender (female)	38% [135]
Diabetes	10% [36]
Hypertension	39% [139]
Hypercholesterolemia	37% [132]
Smoking	25% [91]
Obesity (BMI $\geq 30$ kg/m <sup>2</sup> )	32% [113]
BMI (kg/m <sup>2</sup> )	27.8 [24.9–31.6]
FRS categories	
Low risk (<10%)	63% [223]
Intermediate (10–20%)	23% [80]
High risk (>20%)	14% [51]

**Table 2**

Estimated differences in median PAT volume (cm<sup>3</sup>) between different subgroups of patients. Beside the estimated difference, we reported also 95% confidence intervals (95% CI) of the difference in median levels. Multivariate analysis was adjusted for age, gender, hypertension, hyperlipidemia, diabetes and BMI using median regression.

	<b>Univariate analysis Difference in median PAT volume</b>	<b>Multivariate analysis Difference in median PAT volume</b>
Any CAD vs. no CAD	36.5 [95%CI: 26.9–46.1] cm <sup>3</sup>	19.7 [95%CI: 7.4–31.9] cm <sup>3</sup>
High-risk lesions vs. no high-risk CAD	42.0 [95%CI: 10.7–73.2] cm <sup>3</sup>	39.8 [95%CI: 6.5–73.1] cm <sup>3</sup>
High-risk lesions vs. no CAD	77.0 [95%CI: 42.8–111.1] cm <sup>3</sup>	40.1 [95%CI: 12.1–63.9] cm <sup>3</sup>

**Table 3**

Diagnostic accuracy of derived pericardial adipose tissue (PAT) cut-offs for coronary high-risk lesions. NPV, negative predictive value; PPV, positive predictive value; 95% CI, 95% confidence intervals.

<b>Diagnostic accuracy to detect coronary high-risk lesions</b>					
		<b>Sensitivity [95%CI]</b>	<b>Specificity [95%CI]</b>	<b>NPV [95%CI]</b>	<b>PPV [95%CI]</b>
Entire cohort ( <i>N</i> = 358)					
PAT	74.07 cm <sup>3</sup>	100% [75–100%]	34% [29–40%]	100% [97–100%]	5% [3–9%]
PAT	144.88 cm <sup>3</sup>	62% [32–86%]	83% [79–87%]	78% [73–82%]	12% [5–23%]
Patients with any CAD ( <i>N</i> = 178)					
PAT	74.07 cm <sup>3</sup>	100% [75–100%]	20% [14–27%]	100% [97–100%]	10% [5–16%]
PAT	144.88 cm <sup>3</sup>	62% [32–86%]	77% [70–83%]	96% [91–99%]	17% [8–31%]